Title: Characterizing caspase-1 involvement during esophageal disease progression.

Running head: Caspase-1 importance during Barrett's.

Gillian Barber[1,2], Akanksha Anand[3], Katarzyna Oficjalska[1], James J. Phelan[2], Aisling B. Heeran[2], Ewelina Flis[1], Niamh E. Clarke[2], Jenny A. Watson[4], Julia Strangmann[3], Brian Flood[1], Hazel O'Neill[2], Dermot O'Toole[5], Finbar MacCarthy[5], Narayanasamy Ravi[2,5], John V. Reynolds[2,5], Elaine W. Kay[4], Michael Quante[3], Jacintha O'Sullivan[2], Emma M. Creagh[1 *].

[1]Trinity Biomedical Sciences Institute, School of Biochemistry & Immunology, Trinity College Dublin, Dublin 2, Ireland,

[2]Trinity Translational Medicine Institute, Department of Surgery, Trinity College and St. James's Hospital Dublin, Dublin 8, Ireland,

[3]Department of Internal Medicine, Technical University of Munich, Germany,

[4]Royal College of Surgeons in Ireland and Beaumont Hospital, Dublin 9, Ireland,

[5]National Oesophageal and Gastric Centre, St. James's Hospital, Dublin 8, Ireland.

*__Corresponding author__: Emma M. Creagh, Ph.D

Email: ecreagh@tcd.ie,

Number of figures: 7

Number of tables: 2

Abstract

Barrett's esophagus (BE) is an inflammatory condition and a neoplastic precursor to esophageal adenocarcinoma (EAC). Inflammasome signaling, which contributes to acute and chronic inflammation, results in caspase-1 activation leading to the secretion of IL-1β and IL-18, and inflammatory cell death (pyroptosis). This study aimed to characterize caspase-1 expression, and its functional importance, during disease progression to BE and EAC.

Three models of disease progression (Normal-BE-EAC) were employed to profile caspase-1 expression: (1) a human esophageal cell line model; (2) a murine model of BE; and (3) resected tissue from BE-associated EAC patients. BE patient biopsies and murine BE organoids were cultured *ex-vivo* in the presence of a caspase-1 inhibitor, to determine the importance of caspase-1 for inflammatory cytokine and chemokine secretion.

Epithelial caspase-1 expression levels were significantly enhanced in BE ($p<0.01$). In contrast, stromal caspase-1 levels correlated with histological inflammation scores during disease progression ($p<0.05$). Elevated secretion of IL-1β from BE explanted tissue, compared to adjacent normal tissue ($p<0.01$), confirmed enhanced activity of caspase-1 in BE tissue. Caspase-1 inhibition in LPS-stimulated murine BE organoids caused a significant reduction in IL-1β ($p<0.01$) and CXCL1 ($p<0.05$) secretion, confirming the importance of caspase-1 in the production of cytokines and chemokines associated with disease progression from BE to EAC. Targeting caspase-1 activity in BE patients should therefore be tested as a novel strategy to prevent inflammatory complications associated with disease progression.

Keywords:

Esophageal cancer; Inflammation; Barrett's metaplasia; Inflammasome

Declarations:

Funding

G.B. is supported by a Trinity College 'John Scott Fellowship'. E.F. is an Early Stage Researcher of the EU Horizon 2020 Research and Innovation Programme (Marie Sklodowska-Curie grant agreement No 721906). M.Q. is supported by Deutsche Krebshilfe Max Eder Program.

Conflicts of interest

The authors have no conflicts of interest to declare.

Ethical approval and ethical standards

All research was conducted in accordance with the ethical standards of the institution and country in which the research took place. Murine studies were performed at Technische Universität München (TUM), Germany, in accordance with German Animal Welfare and Ethical Guidelines and approved by the District Government of Bavaria. Ethical approval for patient research was granted by the St. James's Hospital/AMNCH Review Board and Beaumont Hospital Ethics committee. This was concurrent with the 1964 Helsinki declaration and later amendments.

Informed consent

Informed written patient consent was obtained for the use of patient tissue and data prior to inclusion in this study. Publication of this data has additionally been consented. Patient data was pseudo-anonymized prior to sample access.

Availability of data and material

The datasets analyzed during the current study are available in the GEO DataSets repository, NCBI, GSE34619, GSE1420.

Code availability

Not applicable.

Authors' contributions

GB, JOS and EMC are responsible for study conceptualization. GB generated most of the data, assisted by AA, JK and MQ for mice studies; and KO, JP, AH, EF, NC, JW, BF, HON, EK for human studies. DT, FMC, NR, JR contributed clinical specimens. JOS provided resources, supervision and editing. EMC provided funding and supervision. GB and EMC wrote and edited the manuscript. GB is the guarantor of this work and, as such, had full access to all the data in the study and takes responsibility for the integrity of the data and the accuracy of the data analysis.

Abbreviations

CRC, Colitis-associated colorectal cancer; HGD, High-grade dysplasia; IFN-γ, Interferon-gamma; IHC, Immunohistochemistry; IL, Interleukin; LDH, Lactate dehydrogenase; LGD, Low-grade dysplasia; NLRP, Nod-like receptor protein; EAC, Esophageal adenocarcinoma; SCJ, Squamocolumnar junction; TNFα, Tumor necrosis factor alpha.

Précis

Epithelial caspase-1 levels were shown to be selectively upregulated during Barrett's esophagus. Caspase-1 inhibition in Barrett's organoids caused decreased secretion of inflammatory mediators IL-1β and IL-8, suggesting caspase-1 as a therapeutic target.

Introduction

Barrett's esophagus (BE) is an inflammation-driven, pre-neoplastic condition, that is part of a pathological sequence of events predisposing to esophageal adenocarcinoma (EAC) [1, 2]. BE is defined by the replacement of normal squamous epithelium with specialized intestinal metaplasia in the distal esophagus [3]. With disease progression, BE patients may develop features of low- and high-grade dysplasia leading to an increased risk of EAC. Nonetheless, annual risk of developing BE-associated EAC is relatively low at 0.12% [4]. BE patients currently undergo surveillance endoscopies, despite the low rates of progression [3]. As inflammation seems to be a main driver of tumor progression, a better understanding of inflammatory pathways during disease progression is required in order to improve preventive strategies [5].

Caspase-1 is a member of the inflammatory caspase subfamily, which also includes caspase-4 and -5 in humans and caspase-11 in mice [6]. Once activated, caspase-1 is responsible for the direct cleavage and subsequent secretion of the potent inflammatory cytokines IL-1β and IL-18 as part of the canonical inflammasome pathway [7]. The activation of caspase-1 also results in an inflammatory form of cell death, termed pyroptosis, which requires gasdermin D (GSDMD) cleavage [8]. Importantly, caspase-1 activation is an outcome of all inflammasome pathways and is therefore a meaningful indicator for inflammasome-associated inflammation [9]. Caspase-4 and -5 have also been shown to regulate and activate the inflammasome through the non-canonical pathway [6].

BE is an inflammatory condition with elevated levels of chemokines and cytokines, including the neutrophil chemoattractant IL-8 and pro-inflammatory cytokine IL-1β [10, 11]. The influence of inflammatory chemokine and cytokine levels on esophageal disease progression is supported by a recent study which identifies a correlation between increasing neutrophil-lymphocyte ratio (NLR) and neoplastic progression [12]. Furthermore, overexpression of mature IL-1β in the esophagus of mice is responsible for the transgenic BE model, L2-IL-1B [13]. This model highlights the importance of inflammasome pathways in disease development. IL-1β stimulates autocrine signaling to induce BE pathogenesis in the absence of additional risk factors such as bile acid exposure or obesity [13].

The inflammasome sensor proteins NLRP1, NLRP3 and AIM2 are expressed in normal esophageal tissue (www.proteinatlas.org) [14], which are potentially primed through stimuli present in the distal esophagus, leading to enhanced inflammation. This scenario has already been indicated for the NLRP3 inflammasome during BE [15].

We hypothesize that caspase-1-mediated inflammation has a role in the pathogenesis of BE and progression to EAC. We provide evidence that caspase-1 is highly expressed in BE and EAC. *Ex-vivo* inhibition of caspase-1 in BE patient biopsies and in murine BE organoid cultures reduced inflammatory cytokine and chemokine secretion, suggesting that caspase-1 inhibition may represent a novel strategy to prevent inflammatory acceleration of esophageal carcinogenesis.

Materials and methods

Esophageal cell line model of disease

Cell lines Het-1A (normal squamous, RRID: CVCL_3702), QH (CP-A, metaplasia, RRID: CVCL_C451), GO (CP-B, high-grade dysplasia, RRID: CVCL_C452), OE33 (EAC, RRID: CVCL_0471) and SKGT4 (EAC, RRID: CVCL_2195) represent stages of disease progression. All lines, except OE33 and SKGT4 (ECACC), were obtained from ATCC. Het-1A, QH and GO were cultured in BEGM™ Bronchial Epithelial Cell Growth Medium Bullet kit (Lonza). OE33, SKGT4 and THP-1 (RRID: CVCL_0006) cell lines were cultured in RPMI 1640 GlutaMAX™, 10% FBS (Labtech), penicillin-streptomycin (100 U/mL, 100 µg/mL).

Immunoblotting

20 µg protein lysate was run on 12% SDS-PAGE gels, transferred to nitrocellulose, and probed with primary antibodies: anti-caspase-1 (1:500, RRID: AB_2069053); anti-caspase-4 (1:1000, RRID: AB_590743); anti-caspase-5 (1:1000, RRID: AB_590746); anti-β-actin (1:10,000, RRID: AB_262011); followed by HRP-secondary antibody (Jackson ImmunoLabs). Immunoblots were coated with enhanced chemiluminescent (ECL) substrate (Millipore) and developed using the BioRad ChemiDoc™ MP Imaging System. Densitometric analysis was performed using Biorad Image Lab software.

Animal studies

The L2-IL-1B mice used were developed by backcrossing C57BL/6J mice with the mouse model (L2-IL1B, Tg[ED-L2-IL1RN/IL1B]#tcw), which involved targeting IL-1β expression

to the squamous epithelium of the mouse using an Epstein Barr virus L2 promoter [13, 16]. Mice included both genders, were monitored daily and were fed a standard chow diet and water *ad libitum.*

For histology, mice of 4 different age groups (3, 6, 9 and 12 months) representing disease progression were sacrificed by isoflurane overdose (n=5 per group). The esophagus and stomach of L2-IL-1B mice were resected, formalin-fixed (10%) and paraffin-embedded. Histological scoring was performed by an experienced mouse pathologist using a blinded scoring system, using previously established criteria for the influx of immune cells per high-power field, metaplasia, and dysplasia in mice (**Supplementary Table I**) [13]. Inflammation represents a score of all immune cells within a defined area of tissue around the squamocolumnar junction (SCJ), predominantly made up of neutrophil myeloid cells. Metaplasia was assessed through identification of mucous producing cells per gland, and the number of glands with mucous producing cells in the BE area. Dysplasia was assessed by evaluating cellular atypia in the presence of low- and high-grade dysplasia within each gland. Goblet cell ratio was assessed by determining whether each crypt consisting of columnar epithelium was positive or negative for goblet cells. The number of positive crypts was then divided by the total number of crypts, and defined as a percentage (%) [17].

Immunohistochemistry (IHC) was performed using the Vectastain ABC DAB detection kit (Vector Labs) for each mice age group. Sections were deparaffinized, rehydrated and heated antigen retrieval was carried out in 10 mM citrate buffer (pH 6.0, 15 mins). Tissue was blocked (3% BSA, 5% goat serum) and quenched (3% H_2O_2) prior to incubation with anti-caspase-1 (1:50, RRID: AB_1660708), followed by secondary antibody (Vector Labs). Appropriate negative controls (primary antibody omitted) were used. Imaging was performed using Aperio ImageScope viewing software (Leica Biosystems). Scoring was performed by two blinded reviewers (G.B., A.A./E.F.) using a validated semi-quantitative scoring system [5]. Caspase-1

expression was assessed in the epithelium and stroma for percent positivity within the BE region.

Murine BE organoid culture

For organoid culture, cells were taken from the cardia region at the SCJ of 12-month old L2-IL-1B mice and cultured as 3D organoids in Matrigel for 3 weeks, as previously described [18]. Three days prior to harvesting, organoids were pre-treated (1 hour) with caspase-1 inhibitor, WEHD.CHO (50 μM) before 24-hour stimulation with LPS (1 μg/mL). The following day, media was replaced and re-treated with inhibitor and LPS for a further 24 hours. Organoid diameters (μm) were assessed under a light microscope (Zeiss, Axiovert 200M) and analyzed (ImageJ software, Fiji) at 0 h (before treatment), 24 h (during treatment) and 48 h (before harvest).

BE-associated EAC patient tissue

All patients, recruited in the Irish national referral center for upper GI malignancy, were histologically confirmed with BE-associated EAC. Formalin-fixed, paraffin-embedded esophagectomy tissue was retrieved from 32 EAC patients. Defined areas of tumor, islands of BE and adjacent normal mucosa were identified by an experienced histopathologist (E.K.). Tissue microarrays (TMAs) were constructed by taking three tissue cores from each histologically defined tissue area, 4 μm sections were placed on glass slides and heated overnight (37 ºC).

IHC staining was performed using the Leica Bond-III fully automated tissue stainer (Leica Biosystems). Slides were dewaxed before pre-treatment with Bond Epitope Retrieval Solution I. Primary antibody, anti-caspase-1 (1:250 dilution, RRID: AB_2069053) was diluted in Bond Primary Antibody Diluent. Detection and visualization of stained cells was achieved using the

Bond Polymer Refine Detection Kit, using DAB chromogen. Caspase-1 expression was assessed by two blinded reviewers (K.O., J.P.) using a validated semi-quantitative scoring method [19].

Optimization of caspase-1 inhibitor dose in THP-1 cells

Dose response [1, 5, 10 µM] of caspase-1 inhibitor, WEHD.CHO (Trp-Glu-His-Asp-aldehyde, Calbiochem) was carried in the THP-1 cell line (ATCC). WEHD.CHO was chosen for its reported superior caspase-1 specificity [20-22]. THP-1 cells were differentiated to macrophages (10 ng/mL PMA, 48 h), before priming overnight with LPS (1 µg/mL, Sigma). NLRP3 inflammasome activation was induced using ATP (5 mM, 30 min). Caspase-1 activity was determined by quantifying IL-1β secretion in supernatants.

Ex-vivo BE patient explant culture

Histologically confirmed patients with BE were prospectively recruited from St. James's Hospital. BE biopsies were taken from identified areas of metaplasia, while matched adjacent squamous tissue was taken ≥5 cm from the proximal border of the BE region. Two matched biopsies were used per treatment group (4 metaplasia, 4 normal adjacent per patient). *Ex-vivo* matched normal and metaplastic biopsies were cultured in conditioned M199 media and treated with or without caspase-1 inhibitor (10 µM WEHD.CHO dissolved in H_2O, 16 h) before supernatant collection. Inhibitor cytotoxicity was tested by measuring LDH secretion (CytoTox96®, Promega).

Quantification of cytokine secretion

Cytokine levels in supernatants from *ex-vivo* biopsy and murine organoid incubations were quantified by ELISA. For mouse work: IL-1β and IL-6 (MesoScale Diagnostics multiplex) and CXCL1 and CXCL2 (R&D Systems). For human work: IL-1β, IL-6 and TNFα (MesoScale Diagnostics multiplex); IL-8, IL-1α, IFN-γ (BioLegend®); IL-18 (R&D Systems). All assays

were performed as per manufacturer's protocols. Cytokine levels were normalized to total protein content per biopsy/organoid culture (pg/µg).

Statistical analysis

GraphPad Prism 5 software was used for statistical analysis, represented as mean ± SEM. Cell line and mouse experiments were analyzed using One-Way ANOVA followed by Tukey's post hoc test. Clinical data was analyzed using Wilcoxon signed-rank test, One-Way ANOVA followed by Tukey's post hoc test or Two-Way ANOVA followed by Bonferroni's post-test. Correlation analysis using Spearman's correlation coefficient. Statistical significance $p<0.05$.

Results

A cell line model of BE to EAC progression reveals strong expression of caspase-1.

To determine inflammatory caspase expression during disease progression to EAC, an esophageal cell line model representing different stages of disease was employed. The cell lines used were: normal squamous (Het-1A), BE (QH), high-grade dysplasia (GO), well-differentiated EAC (SKGT4), and poorly-differentiated EAC (OE33) (**Fig. 1a**). LPS-stimulated THP-1 cells served as positive control. Expression of the inflammatory caspases-1, -4 and -5 in each cell line was assessed, as all three caspases are capable of regulating inflammasome pathway activities [6]. Immunoblots and densitometry graphs represent relative protein expression of the inflammatory caspases (**Fig. 1b, c**). Caspase-1 was highly expressed in the metaplastic cell line ($p<0.01$), while two EAC cell lines ($p<0.01$) had undetectable levels of caspase-1. Caspase-4 expression was increased in the OAC cell line, OE33, although not significantly. In contrast, no significant differences in caspase-5 expression were detected across the cell lines.

Characterization of disease progression in the L2-IL-1B mouse model of BE.

Observations from the cell line model of progression suggested that caspase-1 may be upregulated during metaplasia. We next sought to identify caspase-1 expression levels during disease development stages in the L2-IL-1B transgenic mouse model of BE [13].

We characterized disease development over time in L2-IL-1B mice using H&E staining. **Fig. 2a** shows representative images of the BE region in groups of mice aged 3, 6, 9 and 12 months**.**

Histological analysis revealed development of inflammation and early evidence of metaplasia at 3 months (**Fig. 2b, c**), with established metaplasia (p<0.001) within 6 months (**Fig. 2c**). At 9 months, histological scores reveal well-established inflammation (p<0.05) and metaplasia (p<0.001), with characteristics of early murine dysplasia (p<0.05) (**Fig. 2a-e**). 12-month old mice reveal the most progressed disease phenotype, distinguished by features of early dysplasia (p<0.01), and reduced goblet cell ratio (p<0.05). Goblet cells are proposed to be protective in BE, while reductions in goblet cell ratios may indicate increased susceptibility to neoplasia [17]. Collectively, the histological scores confirm that L2-IL-1B mice develop metaplasia within 6 months and advance to murine phenotypic dysplastic tissue formations at the SCJ in the following months [13].

Epithelial caspase-1 expression is upregulated during BE metaplasia in L2-IL-1B mice.

To determine caspase-1 expression levels during the establishment of metaplasia, tissue sections from the SCJ of L2-IL-1B mice were IHC stained and scored for caspase-1 expression within the metaplastic regions [5]. Wild-type mice were excluded as no intestinal metaplasia was present in these mice, and therefore received a score of zero. Epithelial caspase-1 levels were substantially upregulated (p<0.001) in 9-month old mice at the SCJ when metaplasia is fully established (**Fig. 3a, b**). Observations from the L2-IL-1B BE model are therefore in agreement with data generated from the cell line model of disease development, where the metaplastic cell line had significant levels of caspase-1, while tumor cell lines had poor expression (**Fig. 1c**). This further supports our hypothesis that epithelial caspase-1 may be playing a key role in driving metaplastic inflammation and early disease. In contrast, stromal expression levels of caspase-1 increased with disease progression with highest values in 9- and 12-month old mice (**Fig. 3c**). This result correlated with histological values for inflammation and dysplasia at the SCJ in L2-IL-1B mice (p<0.05) (**Fig. 3e, f**), suggesting that caspase-1

expressed within inflammatory infiltrates of BE metaplasia regions may contribute to inflammation-associated disease progression.

Metaplastic regions of EAC patient resection tissue display elevated epithelial caspase-1 expression levels.

We next sought to determine whether similar caspase-1 expression patterns occurred during disease progression in EAC patients. TMA's were generated from areas of patient-matched adjacent normal tissue, BE metaplasia and EAC within esophageal resection tissue from 32 patients (**Table I**). The TMAs were stained and scored for caspase-1 expression levels.

Similar to previous observations from the murine and *in-vitro* models, we observed significantly higher levels of epithelial caspase-1 expression in metaplastic tissue ($p<0.01$) compared to normal esophageal tissue, but not in tumor tissue (**Fig. 4a, b**). *CASP1* gene expression was also higher in BE tissue when compared to matched normal gastric cardia (**Supplementary fig. 1**). As expected, stromal caspase-1 expression scores were higher in metaplastic and tumor regions, when compared to less inflamed adjacent normal tissue, although differences were not statistically significant (**Fig. 4a, c**).

Biopsies from BE regions secrete higher levels of inflammatory mediators, compared to adjacent normal biopsies.

Ex-vivo explant culture of BE patient biopsy tissue (metaplastic and matched normal) was subsequently carried out to characterize the inflammatory cytokine secretion profile of metaplastic BE tissue, particularly regarding IL-1β and IL-18, as their secretion is directly dependent on caspase-1. Explant biopsies were taken from previously diagnosed BE patients

(n=10) undergoing routine surveillance endoscopies. Patient characteristics are shown in (**Table II**). For each patient, biopsies were taken from identified areas of metaplasia (x2) and normal squamous epithelium (x2). Analysis of culture supernatants confirmed that BE explant tissues demonstrated higher levels of IL-1β, IL-6, IL-8 and IFN-γ ($p<0.01$), when compared to adjacent normal tissue (**Fig. 5a, c-e**). Elevated levels of these inflammatory cytokines have been reported by other studies [10, 15, 23]. In contrast, levels of IL-18 secretion were reduced ($p<0.01$) in BE explants compared to adjacent normal tissue (**Fig. 5b**). Analysis of pro-*IL1B* and pro-*IL18* mRNA expression in two publicly available BE patient datasets [24, 25] showed that pro-*IL1B* mRNA is significantly increased, while pro-*IL18* mRNA levels are significantly lower in BE tissue, compared to adjacent normal (**Supplementary fig. 2a-d**). These observations suggest that the columnar epithelial cells of metaplastic tissue have a lower constitutive pro-IL-18 expression compared to adjacent normal squamous tissue.

Effect of caspase-1 inhibition on inflammatory cytokine secretion in BE patient biopsies.

To determine the functional role of caspase-1, normal and BE explants (n=10 patients) were cultured in the presence or absence of a tetra-peptide caspase-1 inhibitor (WEHD.CHO). A dose response analysis of WEHD.CHO carried out in activated THP-1 macrophages revealed that caspase-1 activity was optimally inhibited at 10 μM, as indicated by reduced levels of IL-1β secretion (**Fig. 6a**). Analysis of supernatants from the biopsy cultures revealed no significant differences in LDH secretion between WEHD.CHO-treated and -untreated groups, indicating no cytotoxic effect of WEHD.CHO (**Fig. 6b**). Analysis of inflammatory cytokines from the supernatants revealed varying levels of caspase-1 inhibitor efficacy (**Fig. 6c-f**). 50% of patients showed reduced IL-1β secretion, and 60% of patients showed reduced IL-8 secretion, in response to inhibitor treatment (**Fig. 6c, f**). These results highlight the inter-patient variability and heterogeneity associated with patient biopsy analysis.

Further separation of cytokine secretion profiles based on patient obesity status (BMI, obese ≥ 30 kg/m²) revealed that obese BE patients had slightly higher, although not significant, IL-1β and IL-18 secretion levels (**Supplementary fig. 3a, b).** In response to caspase-1 inhibition, 4/6 obese BE patients had reduced IL-1β secretion with no obvious differences observed for IL-18 secretion (**Supplementary fig. 3c, d)**. These results suggest that caspase-1 inhibition may limit inflammation in BE patients, particularly those with obesity. However, inhibitor analysis in a larger BE patient cohort is required for this to be statistically confirmed.

Caspase-1 inhibition limits the secretion of IL-1β and CXCL1 in BE organoid cultures.

To further explore the importance of caspase-1 activity during metaplasia, BE organoids from 12-month old L2-IL-1B mice were cultured and stimulated with LPS in the presence or absence of WEHD.CHO (**Fig. 7**). Representative images of untreated metaplastic organoids are shown at 0, 24 and 48 h (**Fig. 7a**). Although organoid growth plots revealed no significant differences in proliferation between groups (**Fig. 7b**), we observed reduced IL-1β ($p<0.01$) secretion in the presence of the caspase-1 inhibitor in LPS-stimulated organoids (**Fig. 7d**). BE organoids secreted low levels of IL-6, with no significant differences observed between treatment groups (**Fig. 7e**). In contrast, significant secretion of the murine IL-8 orthologs CXCL1 and CXCL2 ($p<0.01$) occurred in response to LPS stimulation (**Fig. 7f, g**). In the presence of the caspase-1 inhibitor, reductions in CXCL2 secretion were not found to be significant, however CXCL1 secretion from stimulated organoids was significantly reduced ($p<0.05$) (**Fig. 7f, g**).

Discussion

This study characterizes the expression of caspase-1 during esophageal disease, confirming that stromal caspase-1 expression correlates with histological inflammation during disease progression (Normal-BE-EAC). A selective over-expression pattern for epithelial caspase-1 during BE metaplasia was identified, and caspase-1 inhibitor experiments suggest that caspase-1 mediates the production of disease-associated inflammatory factors during esophageal disease progression. We and others have observed that inflammation is a main driver of disease progression in BE and therefore anti-inflammatory strategies directed against the inflammasome might emerge as preventative therapies [1, 5].

Although the majority of inflammasome studies have been performed in innate immune cells, active inflammasome complexes have been identified in epithelial cells derived from mucosa including the skin, intestine and lung [26]. A study by Nadatani *et al.* supports our findings, showing that NLRP3 inflammasome activation occurs in LPS-stimulated BE cell lines, but not in normal squamous cells, resulting in IL-1β secretion [15]. A rationale for this observation may be provided by our data, which employed three separate model systems to confirm that caspase-1 expression is significantly higher in BE, compared to normal squamous epithelial cells. Our data suggests that increased availability of caspase-1, which associates with ASC and upregulated NLRP3 following LPS priming, contributes to the increased NLRP3 activity observed in BE epithelial cells.

There are many examples of inflammasome signaling driving inflammation-associated carcinogenesis, identifying caspase-1 as a common instigator and driver of disease [27, 28]. However, inflammasomes are also attributed with roles in anti-tumor immunity during carcinogenesis [29]. In our study, caspase-1 expression was undetectable in the two EAC cell lines used in the cell line disease progression model, while in the murine model epithelial caspase-1 expression levels appeared to decrease once a more dysplastic phenotype had developed. Similar observations have been made in inflamed and tumorigenic colon tissue, where a trend towards elevated epithelial caspase-1 expression in inflamed tissue, but lower levels in tumor tissue from colitis-associated colorectal cancer (CRC) patients was shown [30]. In the context of non-GI adenocarcinomas, caspase-1 expression is also significantly lower in tumor compared to adjacent tissue in both breast and prostate [31, 32]. These observations suggest that tumor-induced suppression of caspase-1 expression, and thus inflammasome activity, may be occurring in established EAC cells, highlighting the complexity of inflammasome signaling during cancer progression.

BE is a mosaic of metaplastic subtypes, displaying significant heterogeneity on a cellular and molecular level. Inflammation is maximal at the SCJ and is characterized by increased levels of IL-1β and IL-8, the expression of which is stimulated by the interaction between immune cells and epithelia at the SCJ [10]. As part of its pro-inflammatory effect, IL-1β induces the expression of IL-8/CXCL1 chemokines [33, 34]. Consistent with metaplastic heterogeneity, data generated from BE patient biopsies were variable in terms of caspase-1 inhibition effects, with observed reduction in IL-1β and IL-8 secretion in 50% and 60% of patients, respectively. However, a trend towards a greater IL-1β reduction in inhibitor-treated obese patient explants, compared to those from non-obese patients was observed. This is an interesting observation, as both BE and EAC risk are strongly related to obesity and weight gain [35, 36]. Additionally,

the Irish National Barrett's Registry has previously reported that approximately 76% of Barrett's patients are overweight or obese [37].

In the transgenic BE mouse model (L2-IL-1B), epithelial CXCL1 and IL-8 have recently been implicated in neutrophil recruitment and accelerated disease progression during a high fat diet [5]. Results from this study show that LPS-stimulated BE organoids produce significant levels of the IL-8 orthologs, CXCL1 and CXCL2, supporting the hypothesis that metaplastic tissue responds to esophageal microbial stimuli in an inflammatory manner, as has recently been suggested [15]. Furthermore, incubation of LPS-stimulated BE organoids in the presence of a caspase-1 inhibitor resulted in significantly reduced IL-1β and CXCL1 secretion, supporting a role for caspase-1 in BE pathogenesis.

In summary, we identify an association between caspase-1 signaling and metaplastic inflammation, which calls into question the therapeutic potential of targeting inflammasome pathways or caspase-1 activity in BE patients. Blocking IL-1 signaling, via Anakinra, Rilonacept or Canakinumab, has been FDA-approved to treat a broad spectrum of diseases, including rheumatoid arthritis, Crohn's disease and type II diabetes [38]. The CANTOS trial revealed significant reductions in lung cancer incidence and cancer mortality in a Canakinumab-treated cohort of patients [39]. Similar to BE and associated EAC, lung cancer is epithelial derived and highly associated with chronic inflammation [2, 40]. It is therefore tempting to speculate that the mechanisms identified in this study could effectively be targeted by these drugs to help limit inflammation-induced acceleration of disease progression in BE patients. However, caution must also be taken, as data also suggests that caspase-1 is actively suppressed within established EAC tissue.

Acknowledgements

We would like to thank members of the gastroenterological and surgical teams in St. James's Hospital and Beaumont Hospital and all patients who gave their consent to partake in this study. The authors thank Glen Byrne for his help with digital images. This research was supported by a Trinity College 'John Scott Fellowship' and an EU Horizon 2020 Marie Sklodowska-Curie ITN 'TRACT', grant agreement No 721906.

Figure legends

Fig. 1

A cell line model of EAC progression reveals strong expression of caspase-1. **a** Cell lines representative of EAC progression: Het-1A (normal squamous), QH (BE), GO (high-grade dysplasia), OE33 and SKGT4 (EAC) and THP-1 (positive control). **b** Western blot analysis and **c** subsequent densitometric analysis (arbitrary units) of inflammatory caspase-1 (45 kDa), caspase-4 (43.2 kDa, 36.7 kDa), and caspase-5 (49.7 kDa, 33.3 kDa) in esophageal cell lines. 20 µg lysate was loaded/well of a 12% SDS-PAGE gel (Biorad). Immunoblots are representative of three independent experiments. Densitometry data represents mean ± SEM (n=3), normalized to loading control, β-actin using Biorad Image Lab software. One-way ANOVA followed by Tukey's post hoc test: $*p<0.05$, $**p<0.01$.

Fig. 2

Characterization of disease progression in the L2-IL-1B mouse model of BE. **a** Representative H&E stained images of the BE region at the SCJ in L2-IL-1B mice at 3 (n=4), 6 (n=5), 9 (n=5) and 12 (n=5) months (Aperio ImageScope, Leica). Arrows: 1) columnar epithelium, 2) well-differentiated goblet-like cells, 3) nuclear misalignment and crowding in dysplastic columnar cells. Magnification 20X, scale bars = 20 µm. **b** Histological scores for inflammation (Scale: 0 = no inflammation, 1 = mild, 2 = moderate, 3 = severe). **c** Histological scores for metaplasia

(Scale: 0 = no metaplasia, 1 = rare mucous cells, 2 = single metaplastic glands, 3 = multiple metaplastic glands). **d** Histological scores for dysplasia (Scale: 0 = no dysplasia, 1 = superficial epithelial atypia, 2 = atypia with granular complexity, 3 = low-grade dysplasia, 4 = high-grade dysplasia). **e** Goblet cell ratio (%) calculated as a percentage of goblet cell positivity within each crypt in the BE region. Data represents mean ± SEM. One-way ANOVA followed by Tukey's post hoc test: *p<0.05, **p<0.01, ***p<0.001.

Fig. 3

Epithelial caspase-1 expression is upregulated during BE metaplasia in L2-IL-1B mice. **a** Representative images of caspase-1 IHC staining in BE regions at the SCJ in L2-IL-1B mice at 3 (n=4), 6 (n=5), 9 (n=5) and 12 (n=5) months. Images taken at 20X magnification, scale bars = 10 µm. Graphs represent cytoplasmic caspase-1 positivity (%) of **b** columnar epithelium and **c** stroma within the BE region. Data represents mean ± SEM. One-way ANOVA followed by Tukey's post hoc test. Correlation of stromal caspase-1 expression (%) verses scores for **d** inflammation and **e** dysplasia. r_s = Spearman's correlation coefficient, *p<0.05, ***p<0.001.

Fig. 4

Metaplastic regions of EAC patient resection tissue display elevated epithelial caspase-1 expression levels. **a** Representative images of caspase-1 IHC staining in epithelial and stromal cells in histologically defined areas of normal, metaplasia and tumor. Magnification 20X (Leica Biosystems). Caspase-1 IHC scores in **b** epithelium (normal, metaplasia and tumor (n = 32, 32, 26, respectively)) and **c** stroma (normal, metaplasia and tumor (n = 28, 32, 30, respectively)). Data represents mean ± SEM. Wilcoxon signed-rank test: **p<0.01.

Fig. 5

Biopsies from BE regions secrete higher levels of inflammatory mediators, compared to adjacent normal biopsies. Matched esophageal biopsies were taken from diagnosed BE patients

(n=10) from BE and adjacent normal regions. Explant biopsies were cultured for 16 hours and culture supernatants were subsequently measured for levels of inflammatory mediators and normalized to total protein: **a** IL-1β, **b** IL-18, **c** IL-6, **d** IL-8, **e** IFN-γ, **f** TNFα and **g** IL-1α (pg/μg). Cytokines were measured using MSD multiplex analysis (a-c) and ELISA (d-g). Data represents mean ± SEM. Wilcoxon signed-rank test: $**p<0.01$.

Fig. 6

Effect of caspase-1 inhibition on inflammatory cytokine secretion in BE patient biopsies. **a** Dose response of caspase-1 inhibitor, WEHD.CHO (Trp-Glu-His-Asp-aldehyde) (1 μM, 5 μM, 10 μM) in the THP-1 cell line. Cells were PMA stimulated (10 ng/mL, 48 h) prior to LPS stimulation (1 μg/mL, 18 h), followed by ATP stimulation (5 mM, 30 min). Graph is representative of three independent experiments. Paired Student's *t* test: $*p<0.05$, $***p<0.001$. **b-f** Matched esophageal biopsy explants were taken from areas of BE and adjacent normal tissue from previously diagnosed BE patients (n=10). Esophageal explants were cultured with or without WEHD.CHO (10 μM) for 16 hours. **b** Cytotoxicity assay measuring LDH levels in supernatants from adjacent normal and BE explants. Data represents mean ± SEM. Secretion of inflammatory mediators **c** IL-1β, **d** IL-18, **e** IL-6 and **f** IL-8 (pg/μg) were measured using MSD multiplex analysis (c, d) and ELISA (e, f). Two-way ANOVA followed by Bonferroni's post-test: non-significant.

Fig. 7

Caspase-1 inhibition limits the secretion of IL-1β and CXCL1 in BE organoid cultures. **a** Representative images of organoid cultures taken at 0, 24 and 48 h. Magnification: 5X. Scale bars: 200 μm. **b** Growth curves (n=3) following treatments at 0, 24 and 48 h. Data is represented as ± SEM. Organoid secretion levels (n=4) were analyzed for **c** LDH **d** IL-1β, **e** IL-6, **f** CXCL1

511 and **g** CXCL2. Data was normalized to total organoid protein (pg/µg). Paired Student's *t* test:

512 **p*<0 05, ***p*<0 01.

References

[1] M. Quante, T.A. Graham, M. Jansen, Insights Into the Pathophysiology of Esophageal Adenocarcinoma, Gastroenterology, 154 (2018) 406-420.

[2] S.L. Picardo, S.G. Maher, J.N. O'Sullivan, J.V. Reynolds, Barrett's to oesophageal cancer sequence: a model of inflammatory-driven upper gastrointestinal cancer, Dig Surg, 29 (2012) 251-260.

[3] S.J. Spechler, R.F. Souza, Barrett's Esophagus, New England Journal of Medicine, 371 (2014) 836-845.

[4] F. Hvid-Jensen, L. Pedersen, A.M. Drewes, H.T. Sorensen, P. Funch-Jensen, Incidence of adenocarcinoma among patients with Barrett's esophagus, N Engl J Med, 365 (2011) 1375-1383.

[5] N.S. Munch, H.Y. Fang, J. Ingermann, H.C. Maurer, A. Anand, V. Kellner, V. Sahm, M. Wiethaler, T. Baumeister, F. Wein, H. Einwachter, F. Bolze, M. Klingenspor, D. Haller, M. Kavanagh, J. Lysaght, R. Friedman, A.J. Dannenberg, M. Pollak, P.R. Holt, S. Muthupalani, J.G. Fox, M.T. Whary, Y. Lee, T.Y. Ren, R. Elliot, R. Fitzgerald, K. Steiger, R.M. Schmid, T.C. Wang, M. Quante, High-Fat Diet Accelerates Carcinogenesis in a Mouse Model of Barrett's Esophagus via Interleukin 8 and Alterations to the Gut Microbiome, Gastroenterology, 157 (2019) 492-506.e492.

[6] E.M. Creagh, Caspase crosstalk: integration of apoptotic and innate immune signalling pathways, Trends in Immunology, 35 (2014) 631-640.

[7] S. Mariathasan, D.S. Weiss, K. Newton, J. McBride, K. O'Rourke, M. Roose-Girma, W.P. Lee, Y. Weinrauch, D.M. Monack, V.M. Dixit, Cryopyrin activates the inflammasome in response to toxins and ATP, Nature, 440 (2006) 228-232.

[8] J. Shi, Y. Zhao, K. Wang, X. Shi, Y. Wang, H. Huang, Y. Zhuang, T. Cai, F. Wang, F. Shao, Cleavage of GSDMD by inflammatory caspases determines pyroptotic cell death, Nature, 526 (2015) 660-665.

[9] D. Karan, Inflammasomes: Emerging Central Players in Cancer Immunology and Immunotherapy, Frontiers in immunology, 9 (2018) 3028-3028.

[10] R.C. Fitzgerald, S. Abdalla, B.A. Onwuegbusi, P. Sirieix, I.T. Saeed, W.R. Burnham, M.J. Farthing, Inflammatory gradient in Barrett's oesophagus: implications for disease complications, Gut, 51 (2002) 316-322.

[11] M.S. Shrivastava, Z. Hussain, O. Giricz, N. Shenoy, R. Polineni, A. Maitra, A. Verma, Targeting chemokine pathways in esophageal adenocarcinoma, Cell Cycle, 13 (2014) 3320-3327.

[12] V.J. Campos, G.S. Mazzini, J.F. Juchem, R.R. Gurski, Neutrophil-Lymphocyte Ratio as a Marker of Progression from Non-Dysplastic Barrett’s Esophagus to Esophageal Adenocarcinoma: a Cross-Sectional Retrospective Study, Journal of Gastrointestinal Surgery, 24 (2020) 8-18.

[13] M. Quante, G. Bhagat, J.A. Abrams, F. Marache, P. Good, M.D. Lee, Y. Lee, R. Friedman, S. Asfaha, Z. Dubeykovskaya, U. Mahmood, J.L. Figueiredo, J. Kitajewski, C. Shawber, C.J. Lightdale, A.K. Rustgi, T.C. Wang, Bile acid and inflammation activate gastric cardia stem cells in a mouse model of Barrett-like metaplasia, Cancer Cell, 21 (2012) 36-51.

[14] F. Ponten, K. Jirstrom, M. Uhlen, The Human Protein Atlas--a tool for pathology, J Pathol, 216 (2008) 387-393.

[15] Y. Nadatani, X. Huo, X. Zhang, C. Yu, E. Cheng, Q. Zhang, K.B. Dunbar, A. Theiss, T.H. Pham, D.H. Wang, T. Watanabe, Y. Fujiwara, T. Arakawa, S.J. Spechler, R.F. Souza, NOD-like receptor protein 3 Inflammasome Priming and Activation In Barrett’s Epithelial Cells, Cellular and molecular gastroenterology and hepatology, 2 (2016) 439-453.

[16] H. Nakagawa, T.C. Wang, L. Zukerberg, R. Odze, K. Togawa, G.H.W. May, J. Wilson, A.K. Rustgi, The targeting of the cyclin D1 oncogene by an Epstein-Barr virus promoter in transgenic mice causes dysplasia in the tongue, esophagus and forestomach, Oncogene, 14 (1997) 1185.

[17] R. Schellnegger, A. Quante, S. Rospleszcz, M. Schernhammer, B. Höhl, M. Tobiasch, A. Pastula, A. Brandtner, J.A. Abrams, K. Strauch, R.M. Schmid, M. Vieth, T.C. Wang, M. Quante, Goblet-cell ratio in combination with differentiation and stem cell markers in Barrett’s esophagus allow distinction of patients with and without esophageal adenocarcinoma, Cancer prevention research (Philadelphia, Pa.), 10 (2017) 55-66.

[18] A. Pastula, M. Middelhoff, A. Brandtner, M. Tobiasch, B. Hohl, A.H. Nuber, I.E. Demir, S. Neupert, P. Kollmann, G. Mazzuoli-Weber, M. Quante, Three-Dimensional Gastrointestinal Organoid Culture in Combination with Nerves or Fibroblasts: A Method to Characterize the Gastrointestinal Stem Cell Niche, Stem Cells Int, 2016 (2016) 3710836.
[19] J.J. Phelan, F. MacCarthy, R. Feighery, N.J. O'Farrell, N. Lynam-Lennon, B. Doyle, D. O'Toole, N. Ravi, J.V. Reynolds, J. O'Sullivan, Differential expression of mitochondrial energy metabolism profiles across the metaplasia-dysplasia-adenocarcinoma disease sequence in Barrett's oesophagus, Cancer Lett, 354 (2014) 122-131.
[20] T.A. Rano, T. Timkey, E.P. Peterson, J. Rotonda, D.W. Nicholson, J.W. Becker, K.T. Chapman, N.A. Thornberry, A combinatorial approach for determining protease specificities: application to interleukin-1β converting enzyme (ICE), Chemistry & Biology, 4 (1997) 149-155.
[21] B. Benkova, V. Lozanov, I.P. Ivanov, V. Mitev, Evaluation of recombinant caspase specificity by competitive substrates, Anal Biochem, 394 (2009) 68-74.
[22] J. Rozman-Pungercar, N. Kopitar-Jerala, M. Bogyo, D. Turk, O. Vasiljeva, I. Stefe, P. Vandenabeele, D. Bromme, V. Puizdar, M. Fonovic, M. Trstenjak-Prebanda, I. Dolenc, V. Turk, B. Turk, Inhibition of papain-like cysteine proteases and legumain by caspase-specific inhibitors: when reaction mechanism is more important than specificity, Cell Death Differ, 10 (2003) 881-888.
[23] M.E. Kavanagh, M.J. Conroy, N.E. Clarke, N.T. Gilmartin, K.E. O'Sullivan, R. Feighery, F. MacCarthy, D. O'Toole, N. Ravi, J.V. Reynolds, J. O'Sullivan, J. Lysaght, Impact of the inflammatory microenvironment on T-cell phenotype in the progression from reflux oesophagitis to Barrett oesophagus and oesophageal adenocarcinoma, Cancer Lett, 370 (2016) 117-124.
[24] M. di Pietro, P. Lao-Sirieix, S. Boyle, A. Cassidy, D. Castillo, A. Saadi, R. Eskeland, R.C. Fitzgerald, Evidence for a functional role of epigenetically regulated midcluster HOXB genes in the development of Barrett esophagus, Proc Natl Acad Sci U S A, 109 (2012) 9077-9082.
[25] E.T. Kimchi, M.C. Posner, J.O. Park, T.E. Darga, M. Kocherginsky, T. Karrison, J. Hart, K.D. Smith, J.J. Mezhir, R.R. Weichselbaum, N.N. Khodarev, Progression of Barrett's metaplasia to adenocarcinoma is associated with the suppression of the transcriptional programs of epidermal differentiation, Cancer Res, 65 (2005) 3146-3154.
[26] P.T. Santana, J. Martel, H.-C. Lai, J.-L. Perfettini, J.M. Kanellopoulos, J.D. Young, R. Coutinho-Silva, D.M. Ojcius, Is the inflammasome relevant for epithelial cell function?, Microbes and Infection, 18 (2016) 93-101.
[27] S.R. Kopalli, T.B. Kang, K.H. Lee, S. Koppula, NLRP3 Inflammasome Activation Inhibitors in Inflammation-Associated Cancer Immunotherapy: An Update on the Recent Patents, Recent Pat Anticancer Drug Discov, 13 (2018) 106-117.
[28] B. Guo, S. Fu, J. Zhang, B. Liu, Z. Li, Targeting inflammasome/IL-1 pathways for cancer immunotherapy, Sci Rep, 6 (2016) 36107.
[29] F. Ghiringhelli, L. Apetoh, A. Tesniere, L. Aymeric, Y. Ma, C. Ortiz, K. Vermaelen, T. Panaretakis, G. Mignot, E. Ullrich, J.L. Perfettini, F. Schlemmer, E. Tasdemir, M. Uhl, P. Genin, A. Civas, B. Ryffel, J. Kanellopoulos, J. Tschopp, F. Andre, R. Lidereau, N.M. McLaughlin, N.M. Haynes, M.J. Smyth, G. Kroemer, L. Zitvogel, Activation of the NLRP3 inflammasome in dendritic cells induces IL-1beta-dependent adaptive immunity against tumors, Nat Med, 15 (2009) 1170-1178.
[30] B. Flood, K. Oficjalska, D. Laukens, J. Fay, A. O'Grady, F. Caiazza, Z. Heetun, K.H. Mills, K. Sheahan, E.J. Ryan, G.A. Doherty, E. Kay, E.M. Creagh, Altered expression of caspases-4 and -5 during inflammatory bowel disease and colorectal cancer: Diagnostic and therapeutic potential, Clin Exp Immunol, 181 (2015) 39-50.
[31] Y. Sun, Y. Guo, Expression of Caspase-1 in breast cancer tissues and its effects on cell proliferation, apoptosis and invasion, Oncol Lett, 15 (2018) 6431-6435.
[32] R.N. Winter, A. Kramer, A. Borkowski, N. Kyprianou, Loss of caspase-1 and caspase-3 protein expression in human prostate cancer, Cancer Res, 61 (2001) 1227-1232.

612 [33] C. Biondo, G. Mancuso, A. Midiri, G. Signorino, M. Domina, V. Lanza Cariccio, N. Mohammadi, M.
613 Venza, I. Venza, G. Teti, C. Beninati, The interleukin-1β/CXCL1/2/neutrophil axis mediates host
614 protection against group B streptococcal infection, Infection and immunity, 82 (2014) 4508-4517.
615 [34] C.-H. Lee, S.-H. Syu, K.-J. Liu, P.-Y. Chu, W.-C. Yang, P. Lin, W.-Y. Shieh, Interleukin-1 beta
616 transactivates epidermal growth factor receptor via the CXCL1-CXCR2 axis in oral cancer, Oncotarget,
617 6 (2015) 38866-38880.
618 [35] A. Kubo, M.B. Cook, N.J. Shaheen, T.L. Vaughan, D.C. Whiteman, L. Murray, D.A. Corley, Sex-
619 specific associations between body mass index, waist circumference and the risk of Barrett's
620 oesophagus: a pooled analysis from the international BEACON consortium, Gut, 62 (2013) 1684-1691.
621 [36] F. Turati, I. Tramacere, C. La Vecchia, E. Negri, A meta-analysis of body mass index and esophageal
622 and gastric cardia adenocarcinoma, Ann Oncol, 24 (2013) 609-617.
623 [37] S.L. Picardo, M.P. O'Brien, R. Feighery, D. O'Toole, N. Ravi, N.J. O'Farrell, J.N. O'Sullivan, J.V.
624 Reynolds, A Barrett's esophagus registry of over 1000 patients from a specialist center highlights
625 greater risk of progression than population-based registries and high risk of low grade dysplasia,
626 Diseases of the Esophagus, 28 (2015) 121-126.
627 [38] C.A. Dinarello, A. Simon, J.W.M. van der Meer, Treating inflammation by blocking interleukin-1 in
628 a broad spectrum of diseases, Nature reviews. Drug discovery, 11 (2012) 633-652.
629 [39] P.M. Ridker, B.M. Everett, T. Thuren, J.G. MacFadyen, W.H. Chang, C. Ballantyne, F. Fonseca, J.
630 Nicolau, W. Koenig, S.D. Anker, J.J.P. Kastelein, J.H. Cornel, P. Pais, D. Pella, J. Genest, R. Cifkova, A.
631 Lorenzatti, T. Forster, Z. Kobalava, L. Vida-Simiti, M. Flather, H. Shimokawa, H. Ogawa, M. Dellborg,
632 P.R.F. Rossi, R.P.T. Troquay, P. Libby, R.J. Glynn, Antiinflammatory Therapy with Canakinumab for
633 Atherosclerotic Disease, New England Journal of Medicine, 377 (2017) 1119-1131.
634 [40] L.A. Borthwick, The IL-1 cytokine family and its role in inflammation and fibrosis in the lung,
635 Seminars in Immunopathology, 38 (2016) 517-534.

636

-

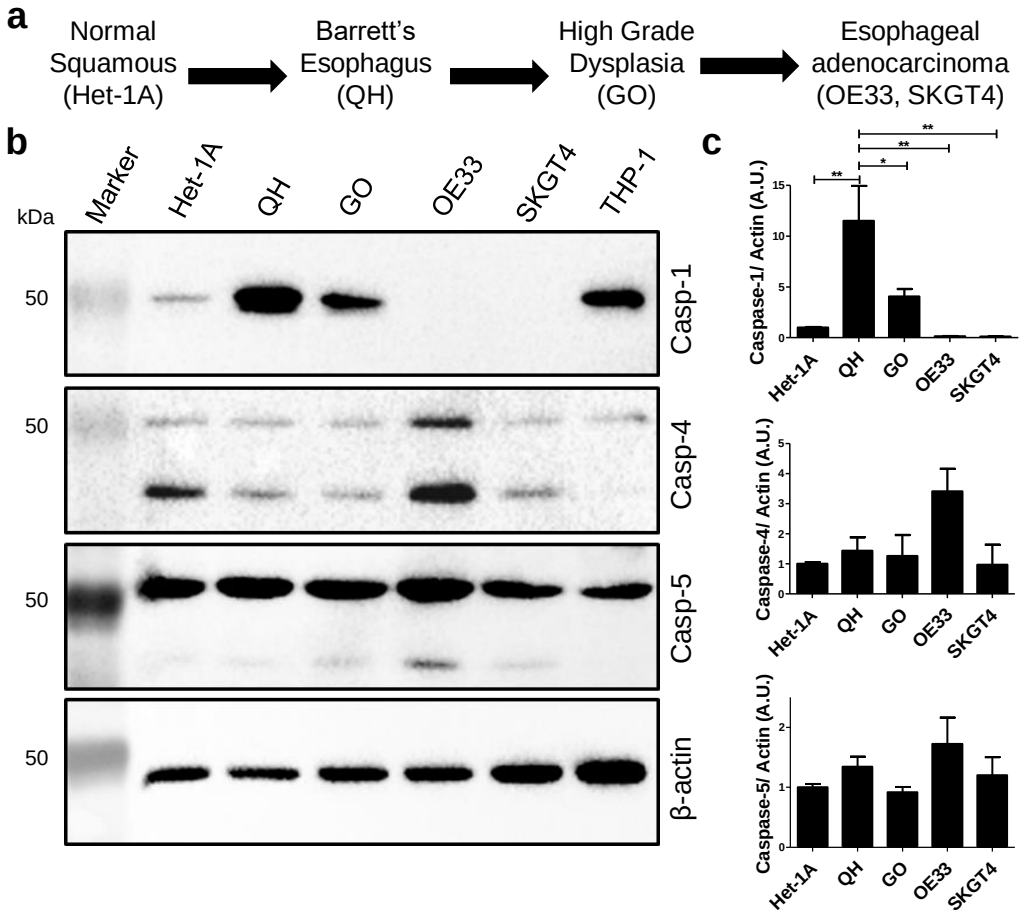
a
Normal Squamous (Het-1A)
Barrett's Esophagus (QH)
High Grade Dysplasia (GO)
Esophageal adenocarcinoma (OE33, SKGT4)
b
kDa
Marker
Het-1A
QH
GO
OE33
SKGT4
THP-1
50
Casp-1
Casp-4
Casp-5
β-actin
c
Caspase-1/ Actin (A.U.)
Caspase-4/ Actin (A.U.)
Caspase-5/ Actin (A.U.)
Het-1A
QH
GO
OE33
SKGT4

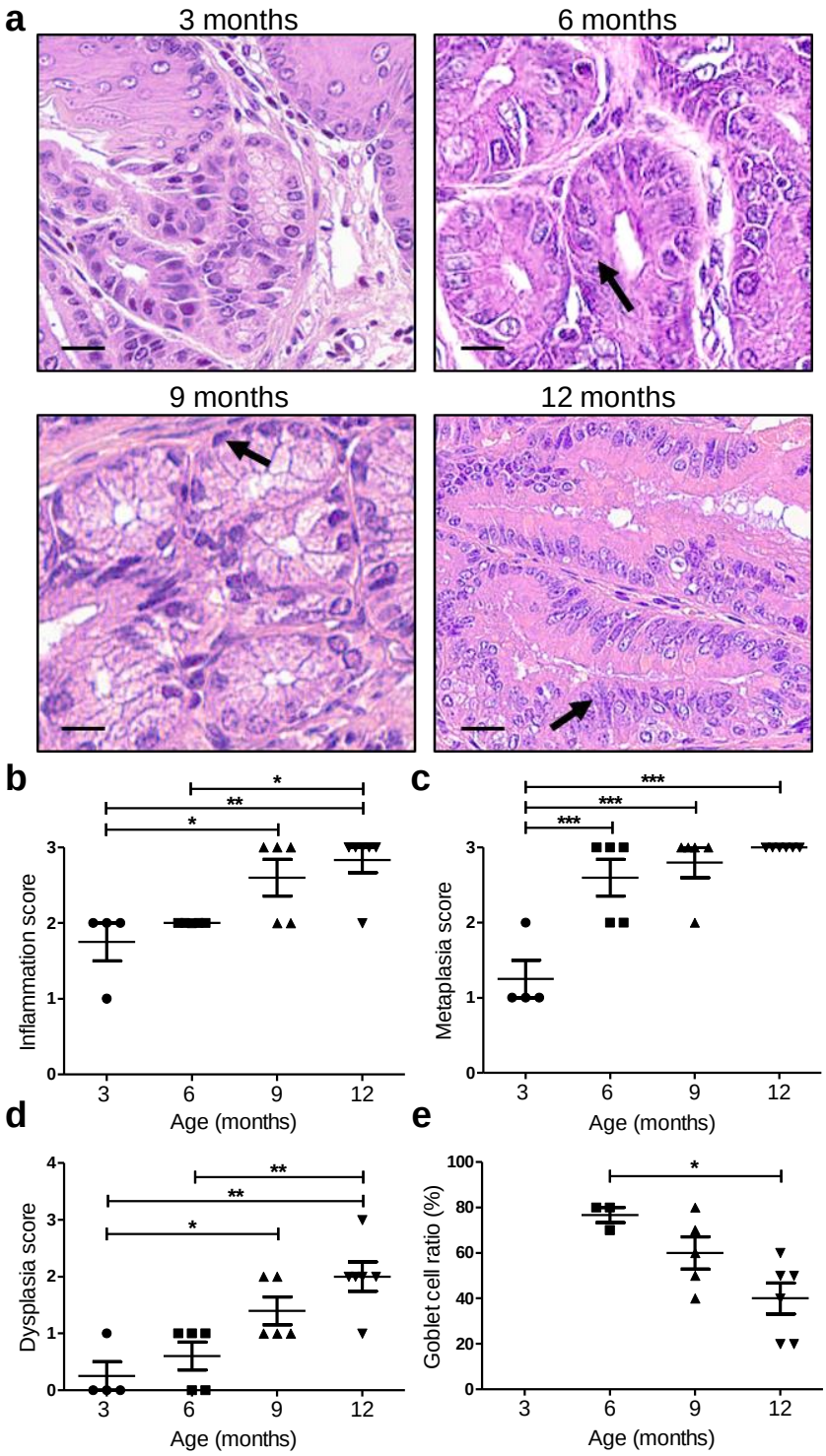
a
3 months
6 months
9 months
12 months
b
Inflammation score
Age (months)
c
Metaplasia score
Age (months)
d
Dysplasia score
Age (months)
e
Goblet cell ratio (%)
Age (months)

-

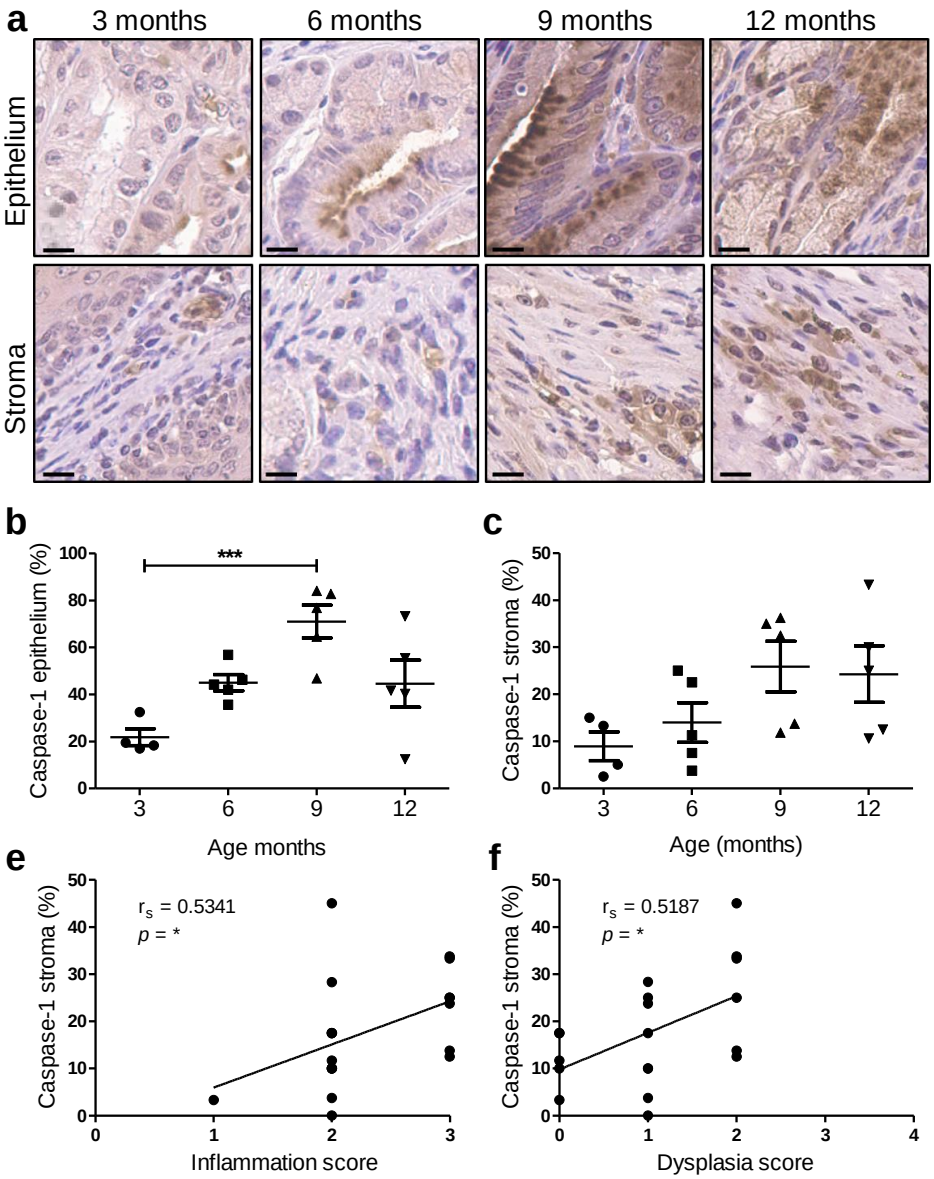
a
3 months
6 months
9 months
12 months
Epithelium
Stroma
b
Caspase-1 epithelium (%)
***
Age months
c
Caspase-1 stroma (%)
Age (months)
e
Caspase-1 stroma (%)
r_s = 0.5341
p = *
Inflammation score
f
Caspase-1 stroma (%)
r_s = 0.5187
p = *
Dysplasia score

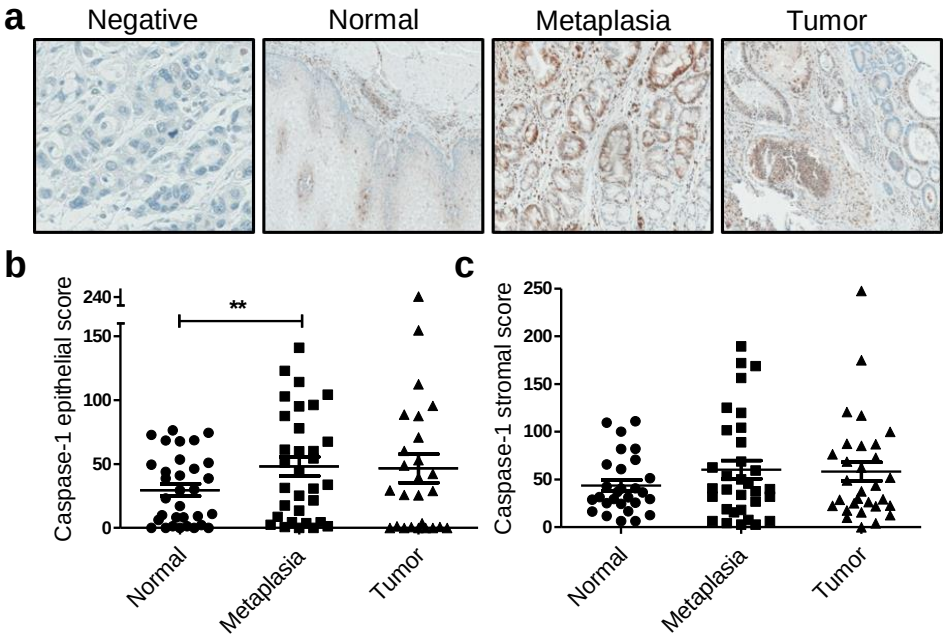
a
Negative
Normal
Metaplasia
Tumor
b
Caspase-1 epithelial score
240
150
100
50
0
**
Normal
Metaplasia
Tumor
c
Caspase-1 stromal score
250
200
150
100
50
0
Normal
Metaplasia
Tumor

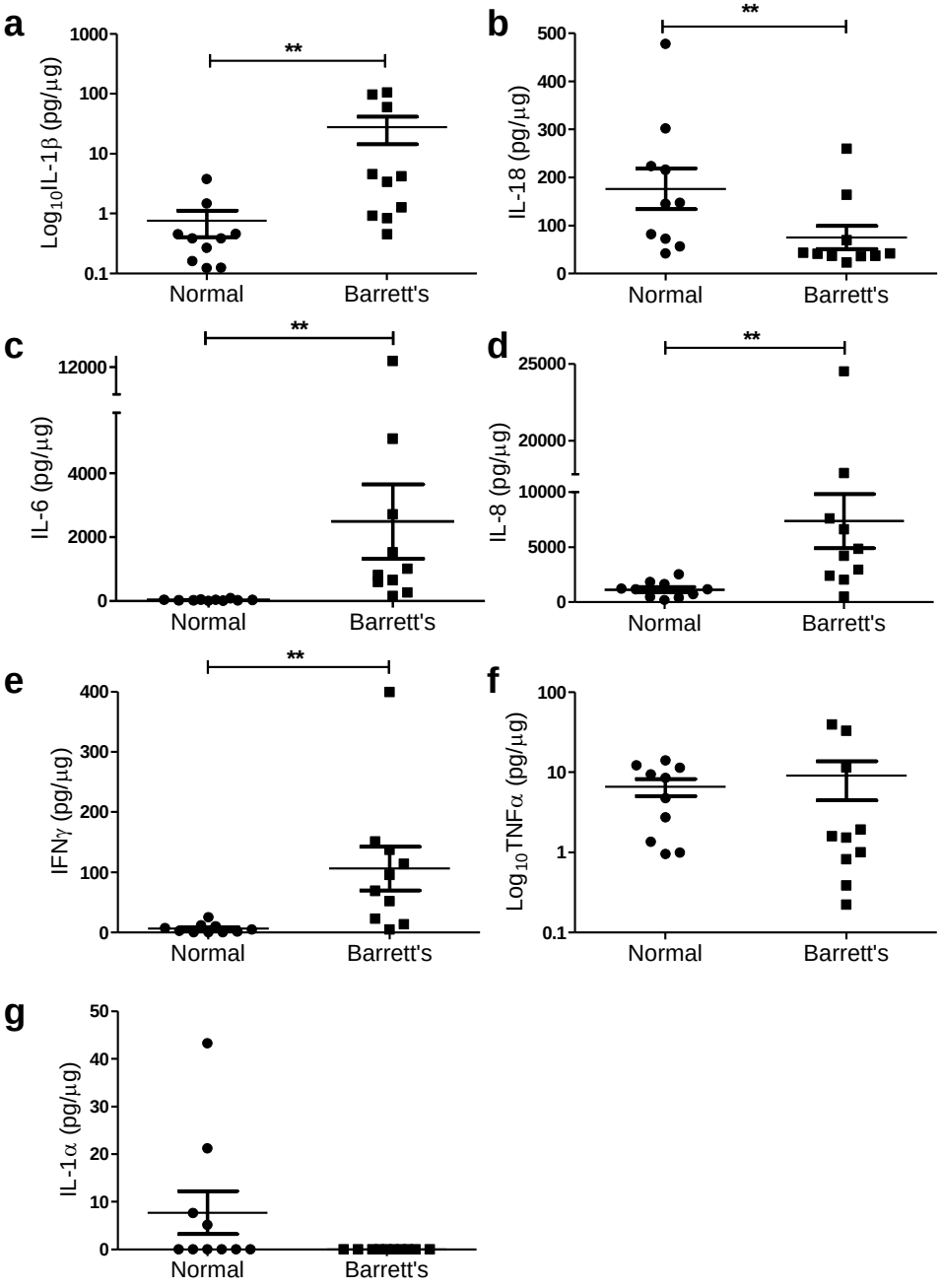
a
Log10IL-1β (pg/μg)
1000
100
10
1
0.1
**
Normal
Barrett's
b
IL-18 (pg/μg)
500
400
300
200
100
0
**
Normal
Barrett's
c
IL-6 (pg/μg)
12000
4000
2000
0
**
Normal
Barrett's
d
IL-8 (pg/μg)
25000
20000
10000
5000
0
**
Normal
Barrett's
e
IFNγ (pg/μg)
400
300
200
100
0
**
Normal
Barrett's
f
Log10TNFα (pg/μg)
100
10
1
0.1
Normal
Barrett's
g
IL-1α (pg/μg)
50
40
30
20
10
0
Normal
Barrett's

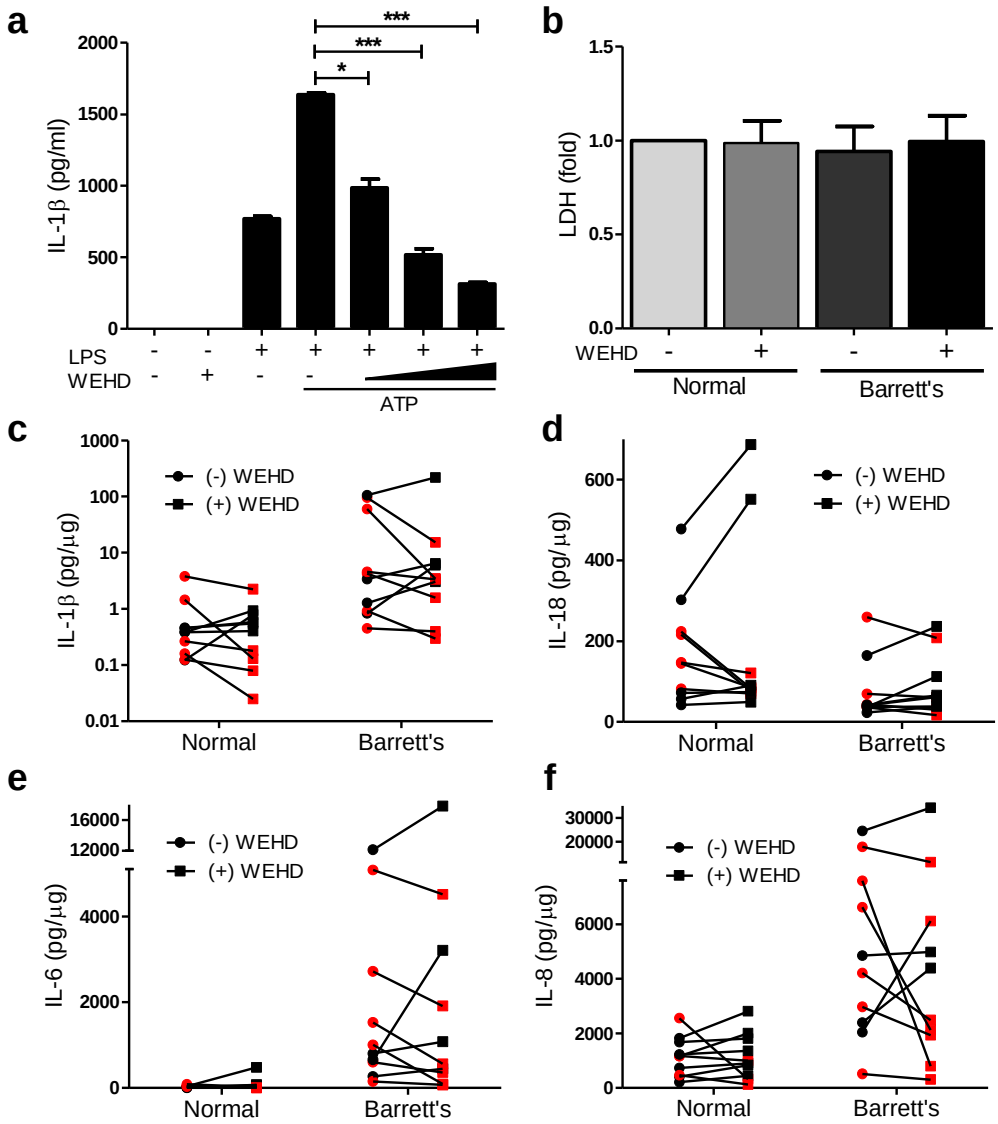
a
IL-1β (pg/ml)
2000
1500
1000
500
0
***
***
*
LPS
WEHD
ATP
b
LDH (fold)
1.5
1.0
0.5
0.0
WEHD
Normal
Barrett's
c
IL-1β (pg/μg)
1000
100
10
1
0.1
0.01
(-) WEHD
(+) WEHD
Normal
Barrett's
d
IL-18 (pg/μg)
600
400
200
0
(-) WEHD
(+) WEHD
Normal
Barrett's
e
IL-6 (pg/μg)
16000
12000
4000
2000
0
(-) WEHD
(+) WEHD
Normal
Barrett's
f
IL-8 (pg/μg)
30000
20000
6000
4000
2000
0
(-) WEHD
(+) WEHD
Normal
Barrett's

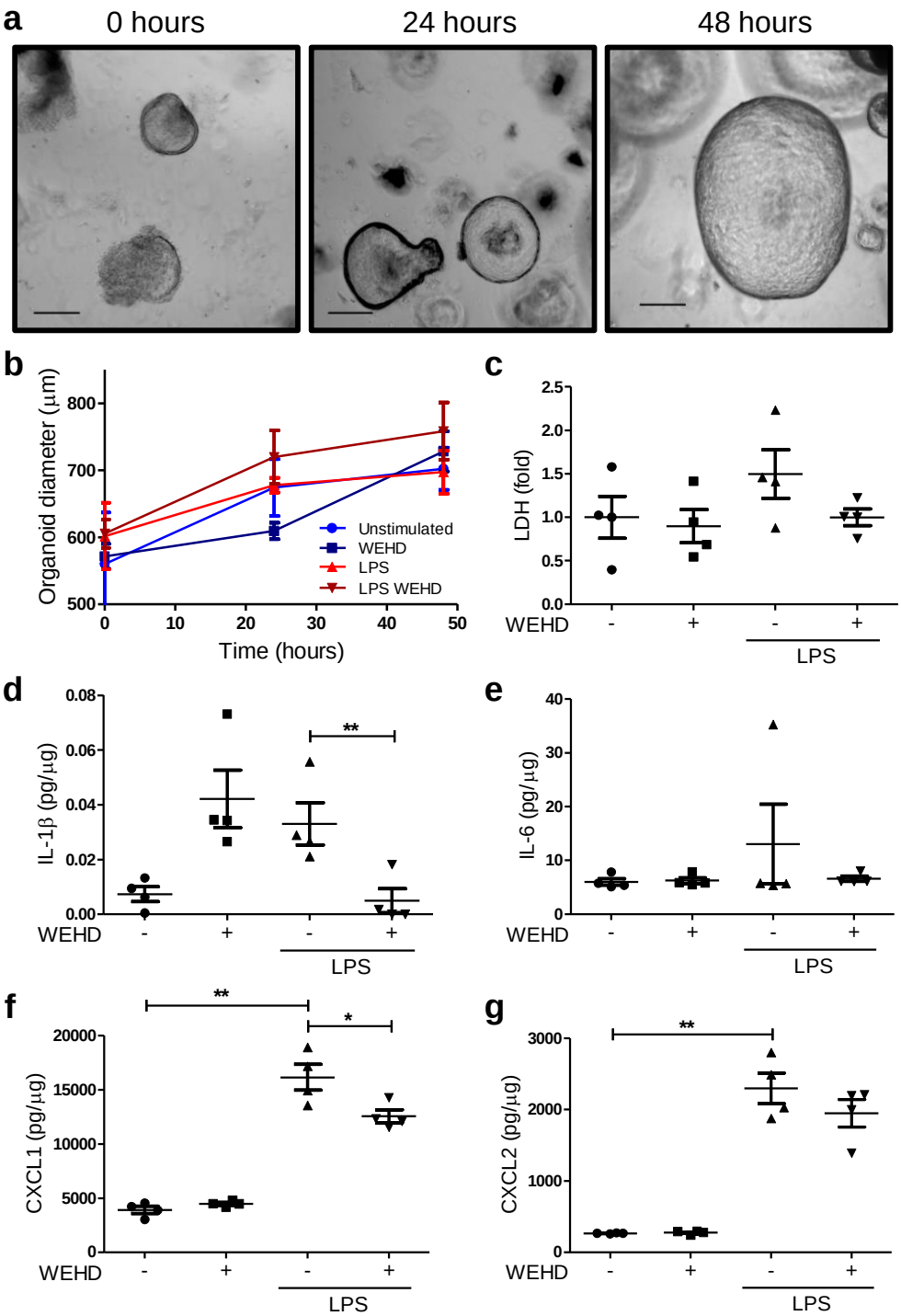
a
0 hours
24 hours
48 hours
b
Organoid diameter (µm)
Time (hours)
Unstimulated
WEHD
LPS
LPS WEHD
c
LDH (fold)
WEHD
LPS
d
IL-1β (pg/µg)
**
e
IL-6 (pg/µg)
f
CXCL1 (pg/µg)
**
*
g
CXCL2 (pg/µg)
**

Table I: Characteristics of EAC patient cohort.

Patient no.	NAT	Differentiation	Grade	Lymph node
1	No	Poor	Not stated	2/8 positive
2	Yes	Moderate	Not stated	Negative
3	No	Moderate	Not stated	19 negative
4	No	Poor	Not stated	11 negative
5	Yes	Moderate	ypT2N0Mx	Negative
7	No	Moderate	Not stated	5/17 positive
9	Yes	Poor	yPT3N1Mx	1 positive
10	No	Well	pT1N0Mx	Negative
11	Yes	Poor	ypT3, N1	3/10 positive
12	No	Moderate	pT3N1Mx	4/6 positive
14	No	Moderate	Not stated	7 negative
15	No	Moderate to poor	TIcN0MX	25 negative
16	No	Moderate	pT3N1Mx	4/14 positive
17	No	Poor	pT3N1Mx	4/10 positive
18	No	-	pT1N0Mx	22 negative
19	Yes	Poor	ypT3N1Mx	1/10 positive
20	Yes	Moderate	yPT2N0Mx	40 negative
21	No	Poor	pT3N0(ITC)Mx	19 negative
22	Yes	-	ypT2N0Mx	5 negative
23	No	Well	pT3N0Mx	10 positive
24	No	Moderate - poor	pT3pN1Mx	5/12 positive
25	No	Poor	pT2N0Mx	14 negative
27	Yes	Moderate	yPT3N1	1/8 negative
28	No	Moderate	ypT3N0Mx	12 negative
29	Yes	Moderate	ypT1N1Mx	2/7 positive
30	Yes	Poor	pT3N1Mx	2/17 positive
31	Yes	Moderate	ypT3N1Mx	3/18 positive
32	Yes	Moderate - poor	pT3N2Mx	6/17 positive
34	Yes	Poor	ypT3N1Mx	1/9 positive
35	No	Moderate - well	pT1	Negative
38	No	Moderate	pT1bN0Mx	Negative
39	No	Moderate	pT1aN0Mx	17 negative

Table II: Barrett's esophagus patient characteristics.

Patient	Age	Sex	Weight (kg)	BMI (kg/m^2)	Prague classification	Vienna grade
1	51	M	111.6	36.03	C0M3	1
2	77	F	89.2	40.72	C1M3	1
3	69	M	74.4	24.43	C12M12	3
4	64	F	89.6	37.78	C5M9	1
5	62	M	82	26.78	C0M5	1
6	77	F	56.3	24.69	C2M3	1
7	57	M	94	28.69	C1M2	1
8	86	M	81.9	28.01	C1M5	1
9	59	M	96.2	33.29	C1M2	4
10	49	M	109	37.64	C0M6	1

Supplementary Table I: Histological scoring method for mice.

H&E score	Inflammation	Metaplasia	Dysplasia
0	No inflammation No immune cell influx	No metaplasia	No dysplasia
1	Mild inflammation Up to 10 immune cells.	Rare mucous cells	Superficial epithelial atypia
2	Moderate inflammation Up to 30 immune cells	Single metaplastic glands	Atypia in granular complexity
3	Severe inflammation More than 30 immune cells	Multiple metaplastic glands	Low grade dysplasia
4	-	-	High grade dysplasia

Previously described by Munch et al. *Gastroenterology*, 2019 [5].

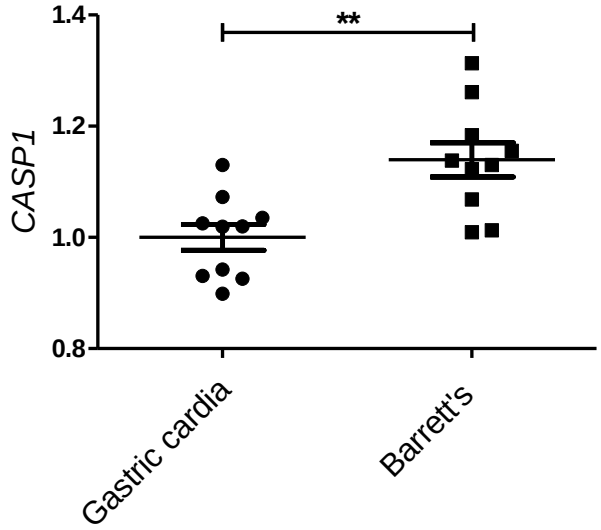

Supplementary fig. 1

Public dataset analysis shows that *CASP1* mRNA levels are significantly higher in Barrett's metaplasia compared to adjacent normal gastric cardia. Graph represents relative *CASP1* mRNA expression in matched patient biopsies from normal adjacent gastric cardia (n=10) and Barrett's oesophagus (n=10) tissue [GSE34619] [24]. Data represents mean ± SEM. Wilcoxon signed-rank test was used to evaluate significant differences between two groups. $^{**}p<0.01$.

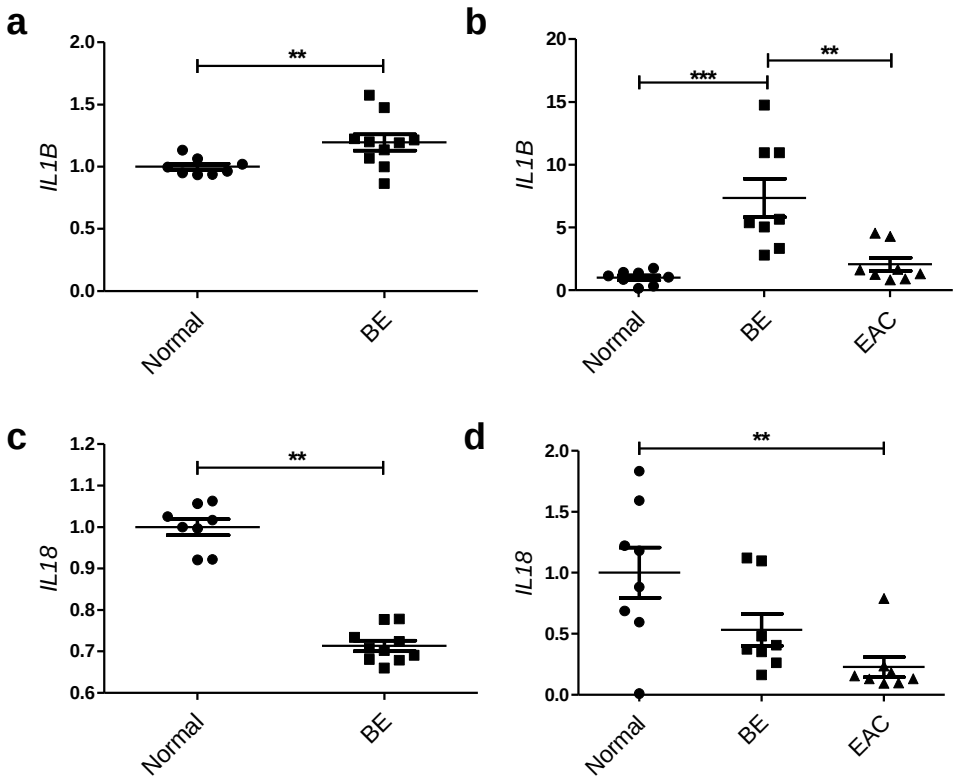

Supplementary fig. 2

Analysis of public datasets reveal IL-1β mRNA levels are upregulated in Barrett's, while IL-18 mRNA levels are decreased in Barrett's and EAC. Graphs represent relative mRNA expression values of pro-*IL1B* and pro-*IL18* analyzed using publicly available datasets. mRNA expression microarray profile of **a** pro-*IL1B* and **c** pro-*IL18* in matched patient biopsies from normal squamous (n=8) and BE (n=10) tissue [24]. Wilcoxon signed-rank test. mRNA expression microarray profile of **b** pro-*IL1B* and **d** pro-*IL18* in matched biopsies (n=8) of normal squamous, BE and EAC [25]. Data represents mean ± SEM. One-way ANOVA followed by Tukey's post hoc test: *p<0.05, **p<0.01, ***p<0.001.

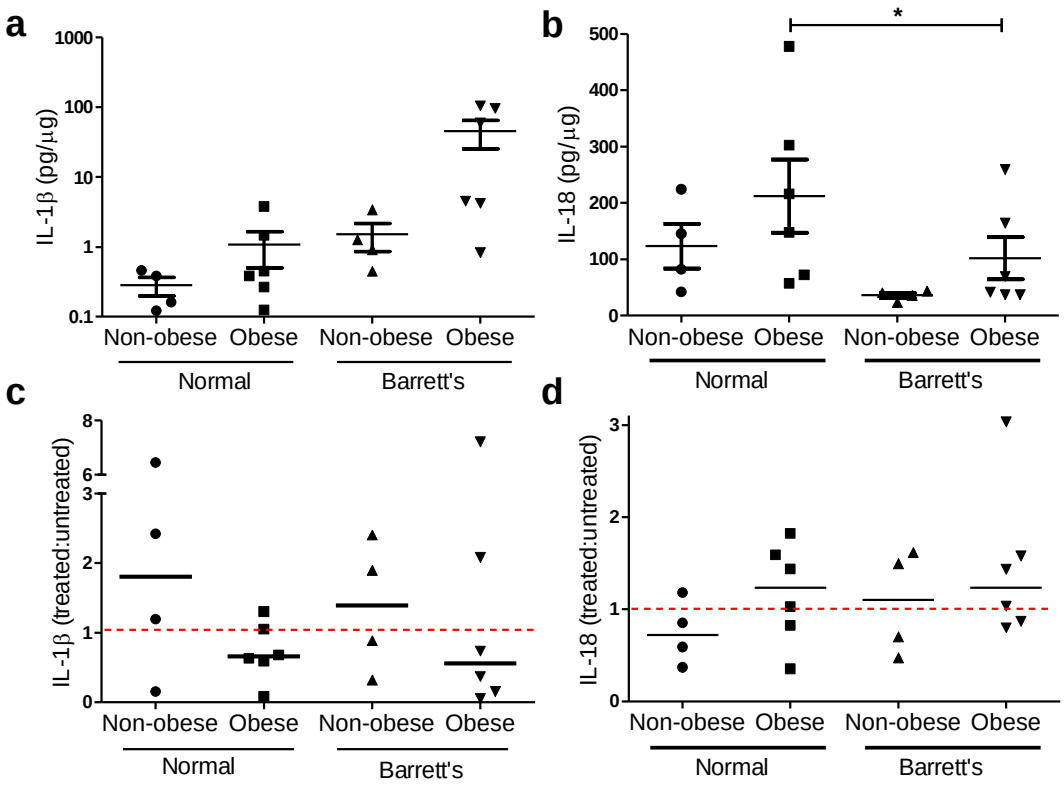

Supplementary fig. 3

Obese BE patients trend towards elevated levels of IL-1β, which are reduced following caspase-1 inhibition. Data is separated based on patient BMI (obese ≥ 30 kg/m²). Secretion levels of **a** IL-1β and **b** IL-18 (pg/μg) from untreated explants. Untreated and treated biopsies are represented by graphs using a WEHD.CHO treated:untreated ratio for **c** IL-1β and **d** IL-18. Data was normalized to total protein of each biopsy and is represented as the median. A ratio <1 (under dashed line) indicates inhibition. Mann Whitney U test comparing non-obese to obese, Wilcoxon signed-rank test for normal verses BE: **p*=0.05.